Scaling laws for single and double electron capture in $A^{q+}+He$ collisions $(q \geqslant Z_A-2)$ at low impact velocities

F. Frémont, C. Bedouet, and X. Husson
Laboratoire de Spectroscopie Atomique, Institut des Sciences de la Matière et du Rayonnement, 6 Boulevard Maréchal, Juin, F-14050 Caen Cedex, France

J.-Y. Chesnel
Hahn-Meitner Institut, Bereich Festkörperphysik, Glienicker Strasse 100, D-14109 Berlin, Germany
(Received 24 November 1997; revised manuscript received 27 January 1998)

We present empirical scaling laws, as a function of the projectile charge state, for single and double electron capture in slow collisions between highly charged ions and He atoms at impact velocities of 0.1 and 0.5 a.u. The fitting parameters are shown to be suitable for predicting the populated states in single and double electron capture. The scaling law for single capture is found to be nearly independent of the projectile velocity in the range 0.1–0.5 a.u. The same fitting procedure is followed for double electron capture at the velocity of 0.5 a.u. since independent monoelectronic transitions, due to electron-nucleus interactions, are dominant. At this velocity, the scaling law for the projectile charge dependence of double electron capture cross sections is found to be similar to that for single electron capture. At the lower velocity of 0.1 a.u., where dielectronic processes caused by the electron-electron interaction gain importance, the charge dependence of double capture cross sections is strongly modified. [S1050-2947(98)01706-5]

PACS number(s): 32.80.Hd, 34.10.+x

I. INTRODUCTION

Electron capture processes involving highly charged ions are of great interest in many fields of physics such as controlled-thermonuclear fusion [1] and astrophysical plasmas [2]. The main directions of these charge-exchange studies have been oriented towards understanding the basic physical mechanisms governing the capture process [3–8]. Theoretical [3,4] and experimental [5–7] methods were developed to determine cross sections for total electron capture and cross sections for producing specific states (partial cross sections).

Particular attention has been devoted to the study of atomic collisions at low impact velocities v (smaller than the classical velocity of the target electrons involved in the capture). For *single* electron capture in collisions of highly charged ions on atomic targets, energy gain spectroscopy and photon spectroscopy (see, for example, [9–12]) have been used extensively to measure with good accuracy the corresponding total and partial cross sections. In parallel, theoretical methods, such as the classical trajectory Monte Carlo model [13], the classical over-barrier model [14], the Landau-Zener model [15], and molecular expansion close-coupling methods [16], have been developed. From such experimental and theoretical works, the main features for single charge exchange (total and partial cross sections) have been explained over a large range of impact velocities [9].

The situation is quite different for multiple electron capture. This is partly due to the fact that the number of active electrons involved is larger, leading to a more complex, many-body problem. The second difficulty lies in the high number of molecular states necessary to describe the collision. In order to reduce these difficulties, experiments [7,17,18] and calculations [16] were devoted to *double* electron capture from a helium target (two active electrons). The helium atom is an interesting target because it is easily prepared in collision experiments and its electronic structure is the simplest one for a theoretical treatment of double capture.

Nevertheless, it should be emphasized that a collision system involving two active electrons forms a complex four-body system whose analysis is still a challenge for the following two reasons.

(i) The mechanisms that are responsible for capture are still under debate [17,19]. Typically, two kinds of interactions are invoked to describe double charge transfer. These mechanisms are illustrated in Fig. 1, which shows the orbital energies for the $C^{6+}+He$ system. First, the electron-nucleus interaction causes a two-step mechanism involving monoelectronic processes. For the example of $C^{6+}+He$ collisions, crossings occur between the He $1s$ orbital and a few orbitals of carbon, where the electrons from He can be transferred independently of each other. Then configurations of near equivalent electrons $nln'l'$ (n and n' ranging from 2 to 4) are produced (Fig. 1). The electron-nucleus interaction is found to be dominant at velocities around 0.5 a.u. [8]. Second, the small residual electron-electron interaction that is not incorporated in the independent particle model produces dynamic electron-correlation effects referred to as dielectronic processes [8]. As illustrated in Fig. 1 for $C^{6+}+He$ collisions, this dynamic electron correlation is likely to create configurations of nonequivalent electrons $nln'l'$ ($n' \gg n$) where one electron is transferred into the $2l$ orbital of carbon, while the second electron is excited into a high-lying Rydberg orbital (e.g., $6l'$) [17,20]. These dielectronic processes were found to play a decisive role at very low velocities [21,22].

(ii) Agreement between different theories is quite poor [3,4]. Discrepancies occur also between theory and experi-

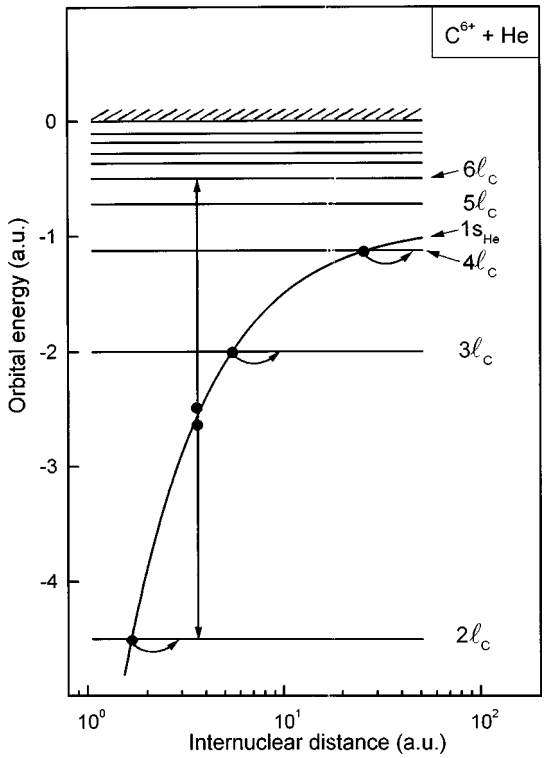

FIG. 1. Diagram of orbital electron energies for the $(C+He)^{6+}$ system showing uncorrelated (inclined arrows) and correlated (vertical arrows) double electron capture. These processes produce configurations of (quasi) equivalent and nonequivalent electrons, respectively.

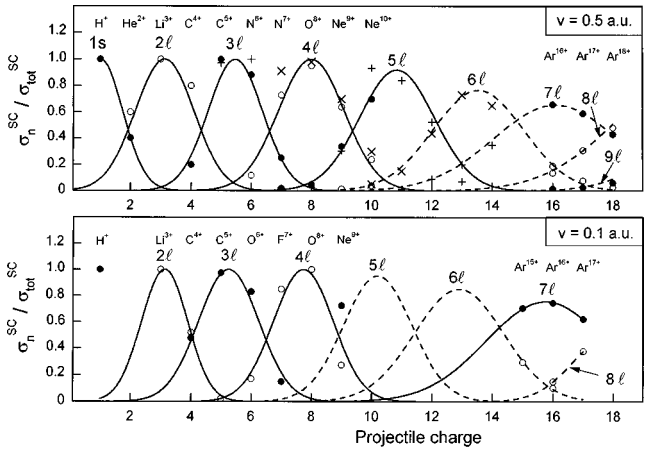

FIG. 2. Experimental cross sections σ_n^{SC} for producing a given n state relative to the total single capture cross sections σ_{tot}^{SC} as a function of the projectile charge in $A^{q+}+He$ collisions (odd n, solid circles; even n, open circles). Collision velocities of about 0.5 and 0.1 a.u. are represented in the top and bottom figures, respectively. Gaussian curves (solid lines) are used to fit the experimental data. Calculations using a multichannel Landau-Zener model [27] for a projectile velocity of 0.5 a.u. are compared with the experimental data (odd n, crosses; even n, pulses). Dashed Gaussian lines extrapolate experiment for n values larger than 5. The data are taken from the following references: for $v\approx 0.5$ a.u., $q=1$ [28], $q=2$ [47], $q=3$ [30], $q=4$ [32], $q=5$ [33], $q=6$ [34], $q=8$ [35], $q=7,9,16,17$ [37], and $q=10,18$ [36]; for $v\approx 0.1$ a.u., $q=1$ [28], $q=3$ [30], $q=4$ [32,22], $q=5$ [32,33], $q=6-8$ [12], $q=9$ [48], and $q=15-17$ [49].

ment for the velocity dependence of the cross sections [20]. Although relative cross sections were extensively measured (see, for example, [17–20]), absolute cross sections are missing in most of the experiments.

However, attempts were made to find general trends and scaling behaviors of single and multiple capture cross sections. Müller and Salzborn [23] concentrated their effort on total single capture cross sections in a large velocity range. Hence it was possible to reveal basic features of charge transfer collisions with multielectron targets. Iwai *et al.* [24] reported one-electron capture cross sections for highly charged ions in collisions with helium at impact energies lower than $3q$ keV ($v<0.3$ a.u.) (q is the charge of the projectile). Absolute cross sections were measured as a function of projectile charge q and compared with a classical one-electron model [24]. Very recently, semiempirical scaling laws were formulated for absolute cross sections for multiple electron capture from different targets (He, Ar, and Xe) [25].

Apart from these works, there is still a considerable need for additional studies in order to understand many important features. For example, only little is known about *partial* cross sections for double electron capture. In the present work, we investigate double electron capture in the collisions

$$A^{q+}+\mathrm{He}(1s^2)\rightarrow A^{(q-2)+}(nln'l')+\mathrm{He}^{2+}, \qquad (1)$$

where $q\geqslant Z-2$ and Z is the atomic number of the ion A^{q+} [26].

In this paper single electron capture is first reviewed. The main attention is devoted to partial cross sections σ_n for populating a state of the projectile with principal quantum number n. From the experimental data, the ratios σ_n/σ_{tot} (σ_{tot} is the sum of the partial cross section over n) are determined as a function of the projectile charge. A simple scaling law is deduced and compared with calculations using the Landau-Zener model [27]. Then an analogous procedure is followed for the experimental double capture data in order to obtain a similar scaling law. The present study is divided into two parts. The velocity range around 0.5 a.u. is explored, where monoelectronic processes are dominant [17]. Details of the results are discussed in conjunction with the capture mechanisms for particular systems investigated previously. Then we focus on lower velocities (~ 0.1 a.u.) where dielectronic processes gain importance [18].

II. SINGLE ELECTRON CAPTURE

Figure 2 and Table I show experimental single capture ratios $\sigma_n^{SC}/\sigma_{tot}^{SC}$ obtained at collision velocities of about 0.5 and 0.1 a.u., as a function of the projectile charge q. The quantity σ_n^{SC} is the cross section for producing the singly excited states $A^{(q-1)+}(nl)$ during the collision $A^{q+}+He$. The quantity σ_{tot}^{SC} is the total cross section for single electron transfer from the target onto the projectile, i.e., the sum of the cross sections σ_n^{SC} over n. Many experiments were performed for charges $q\leqslant 10$ [28–36]. For higher charges, only a few results exist. For example, in the range 11–15, to our knowledge, no data are available. Very recently, measurements using recoil-ion momentum spectroscopy were per-

TABLE I. Experimental cross sections σ_n^{SC} $(n=2-5)$ for producing a given n state relative to total single capture cross sections σ_{tot}^{SC} in $A^{q+}+He$ collisions $(q=4-7)$ at the velocity $v\approx 0.5$ a.u. In the last row the total single capture cross sections σ_{tot}^{SC} deduced from the scaling law formulated in Ref. [25] are given. $q=4$ [32], $q=5$ [33], $q=6$ [34], and $q=7$ [37].

	$\sigma_n^{SC}/\sigma_{tot}^{SC}$			
n	$q=4$	$q=5$	$q=6$	$q=7$
2	0.8	0	0	0
3	0.2	1	0.88	0.25
4	0	0	0.12	0.73
5	0	0	0	0.02
σ_{tot}^{SC} $(10^{-15}$ cm$^2)$	1.8	2.2	2.7	3.1

formed for Ar^{q+} projectiles involving charges from 16 to 18 [36,37].

From Fig. 2 it is seen that single electron capture is quite selective at both velocities (0.1 and 0.5 a.u.), especially in the case of projectile charges lower than 6. In this range of charges, the number of n states produced by single electron capture with significant probability does not exceed 2. For example, single capture populates only the states $n=3$ and 4 in $N^{6+}+He$ collisions [34] (Fig. 2). Moreover, each n state is populated within a restricted range of projectile charge q. Hence, from the available data at both velocities, it is possible to extract charge distributions for given n states. In particular, for values of the principal quantum number n ($n=2-5$ and 7), Gaussian curves were used to fit the experimental ratios $\sigma_n^{SC}/\sigma_{tot}^{SC}$ shown in Fig. 2. As a function of the charge q, each ratio $\sigma_n^{SC}/\sigma_{tot}^{SC}$ was written as

$$\sigma_n^{SC}/\sigma_{tot}^{SC}=a_0(n)\exp\{-[q-q_{max}(n)]^2/[\Delta q(n)]^2\}, \quad (2)$$

where $a_0(n)$, $q_{max}(n)$, and $\Delta q(n)$ are fitting parameters. The quantities $a_0(n)$ and $q_{max}(n)$ are the amplitude and the center of the charge distribution, respectively, and $\Delta q(n)$ is the reduced width. The center $q_{max}(n)$ characterizes the most favorable charge for populating orbitals nl of the projectile. The amplitude $a_0(n)$ and the width $\Delta q(n)$ take into account the selectivity of the single capture process. The values obtained from the fits are listed in Table II.

For both projectile velocities, the principal quantum number n increases with the center $q_{max}(n)$ of the Gaussian curves (Table II and Fig. 2). Also, for $n\leqslant 4$ the amplitude $a_0(n)$ has a value of nearly unity, indicating an extreme selectivity in collisions involving projectile charges close to $q_{max}(n)$, where only a unique final state is produced $(\sigma_n^{SC}/\sigma_{tot}^{SC}\sim 1)$. However, for higher-$n$ values, $a_0(n)$ decreases (0.7 for $n=7$) since the selectivity of single electron capture is reduced when the projectile charge is larger than 9 (Fig. 2). Accordingly, the width $\Delta q(n)$ of the charge distribution increases with increasing n (Table II). This reduction of selectivity results from the decreasing difference between the binding energies of the n states when high-n values are involved. This characteristic feature has already been pointed out for $A^{q+}+H$ collisions [9].

From the knowledge of the quantities $a_0(n)$, $q_{max}(n)$, and $\Delta q(n)$, the scaling law given in Eq. (2) can be improved using the fitting functions

$$q_{max}(n)=q_0 n^{\alpha}, \quad (3)$$

$$\Delta q(n)=\Delta q_0+\Delta q_1 n^{\beta}, \quad (4)$$

$$a_0(n)=\exp[-(n-4)/t] \quad (\text{with } n\geqslant 4), \quad (5)$$

where q_0, α, Δq_0, Δq, β, and t are fitting constants. These parameters are given in Table III. Since Fig. 2 shows that $q_{max}(1)=1$, the quantity q_0 is close to unity. Furthermore, the amplitude a_0 is constant and equal to unity for n values ranging from 1 to 4 (Fig. 2 and Table II). Within uncertainties, the parameters deduced from the fits remain constant in the whole velocity range presently studied. The fitting parameters given in Table III were used to perform extrapolations for higher-n values $(n=6-9)$. It is seen that the experimental data are well represented by the corresponding Gaussian curves (dashed curves in Fig. 2). Furthermore, the use of these additional fitting parameters (Table III) is likely to allow the prediction with good approximation of the ratios $\sigma_n^{SC}/\sigma_{tot}^{SC}$ for projectile charges larger than those presently studied.

It is of interest to compare the above-described charge distributions with model calculations. Hence calculations us-

TABLE II. Values of the fitting parameters of the Gaussian curves [Eq. (2)] characterizing the charge distribution in single capture for $A^{q+}+He$ collisions (Fig. 2) at projectile velocities of 0.1 and 0.5 a.u., as a function of the principal quantum number n populated during the collision. The uncertainties result from the standard deviation of the fitting procedure.

	q_{max}		Δq		a_0	
n	0.5 a.u.	0.1 a.u.	0.5 a.u.	0.1 a.u.	0.5 a.u.	0.1 a.u.
1	1	1	1.0 ± 0.3		1	1
2	3.1 ± 0.2	3.4 ± 0.2	1.4 ± 0.2	1.2 ± 0.3	1	1
3	5.5 ± 0.3	5.5 ± 0.2	1.3 ± 0.1	1.3 ± 0.2	1	1
4	7.9 ± 0.3	7.7 ± 0.2	1.6 ± 0.1	1.4 ± 0.2	1	1
5	10.7 ± 0.4		1.7 ± 0.2		0.9 ± 0.1	
6			2.1 ± 0.2			
7	16.4 ± 0.5	15.8 ± 0.2		2.8 ± 0.2	0.7 ± 0.1	0.8 ± 0.1

TABLE III. Fitting parameters for q distributions following single (SC) and double (DC) electron capture in collisions of $A^{q+}+\mathrm{He}$ at velocities of 0.1 and 0.5 a.u. The experimental ratios $\sigma_n^{\mathrm{SC}}/\sigma_{\mathrm{tot}}^{\mathrm{SC}}$ and $\sigma_n^{\mathrm{DC}}/\sigma_{\mathrm{tot}}^{\mathrm{DC}}$ are characterized, for each n value, by a Gaussian curve centered at $q_{\max}(n)=q_0 n^{\alpha}$. The width and the amplitude of the corresponding Gaussian curves are obtained as $\Delta q(n)=\Delta q_0+\Delta q_1 n^{\beta}$ and $a_0(n)=\exp[-(n-4)/t]$, respectively.

		Fitting parameters					
Capture	v (a.u.)	q_0	α	Δq_0	Δq_1 ($\times 10^2$)	β	t
SC	0.5	1.3±0.1	1.3±0.1	1.1±0.1	2.3±0.5	2.1±0.6	8.2±1.6
SC	0.1	1.4±0.1	1.3±0.1	1.1±0.2	1.0±2.0	2.6±0.7	11.5±2.3
DC	0.5	1.9±0.1	1.3±0.1	1.5	1.1	3.4	

ing the multichannel Landau-Zener model [27] were performed for a projectile velocity of 0.5 a.u. The calculated ratios $\sigma_n^{\mathrm{SC}}/\sigma_{\mathrm{tot}}^{\mathrm{SC}}$ are also shown in Fig. 2 as a function of q ($5\leqslant q\leqslant 14$) for n values up to 7. These results agree well with the experimental data and the same projectile charge dependence is obtained. Moreover, these calculated values are quite consistent with more sophisticated calculations [33,38,39,50].

III. DOUBLE ELECTRON CAPTURE

The rather good agreement between experiment and the model calculations (Fig. 2) suggests that double electron capture can be parametrized in a similar manner if the two capture events are independent. At velocities around 0.5 a.u., double capture principally occurs by means of monoelectronic processes, giving rise to two independent one-electron transitions [8,17]. Thus charge distributions similar to those for single electron capture are expected for double electron capture at $v=0.5$ a.u.

A. Charge distribution at 0.5 a.u.

Experimental ratios $\sigma_n^{\mathrm{DC}}/\sigma_{\mathrm{tot}}^{\mathrm{DC}}$ for double capture are shown in Fig. 3 (see also Table IV). The cross section σ_n^{DC} is defined as the sum over the quantum numbers n',l,l' of the cross sections $\sigma_{nln'l'}^{\mathrm{DC}}$ for producing doubly excited states due to the configurations $nln'l'$, with $n'\geqslant n$. The quantity $\sigma_{\mathrm{tot}}^{\mathrm{DC}}$ is the total cross section for double electron transfer from the target onto the projectile. A detailed analysis of double capture is more restricted than for single capture due to the low number of experimental data points. Published results are available predominantly for projectile charges smaller than 11. For the particular charges $q=7$ and 8, we performed additional measurements using Auger electron spectroscopy and the results are also shown in Fig. 3. Analysis of the $N^{7+}+\mathrm{He}$ system shows that the configuration series $2ln'l'$ ($n'\geqslant 3$) represents ~10% of the total double capture (Table IV). This result is different from that obtained in Ref. [40], where the configurations $2ln'l'$ were not observed. However, the present value of 10% is confirmed by measurements using recoil-ion momentum spectroscopy [41].

In addition, we have conducted measurements for higher projectile charges by using Ar^{14+} and Ar^{16+} ions colliding with He. The spectra show that the series $4ln'l'$ ($n'\geqslant 4$) and $5ln'l'$ ($n'\geqslant 5$) are mainly populated. It is noted that Ar^{14+} has a charge of $Z-4$, i.e., the ion has a $1s^2 2s^2$ core. Nevertheless, due to the large value of Z, the influence of the core is neglected in the first approximation.

A fit procedure similar to that described above for single electron capture was applied to obtain scaling laws for the charge dependence of double electron capture. First, Gaussian curves similar to those given in Eq. (2) were used to fit the experimental ratios $\sigma_n^{\mathrm{DC}}/\sigma_{\mathrm{tot}}^{\mathrm{DC}}$ shown in Fig. 3. The values obtained for the fitting parameters $q_{\max}(n)$ and $\Delta q(n)$ are listed in Table V. The reasonable value of unity was taken for the amplitude $a_0(n)$. Then the characteristic quantities $q_{\max}(n)$ and $\Delta q(n)$ were expressed using relations (3) and (4). The corresponding fitting constants obtained are listed in Table III.

A comparison between Figs. 2 and 3 shows a similar behavior for double capture at $v=0.5$ a.u. to that for single capture. The most favorable charge for producing a given series $nln'l'$ increases with respect to the quantum number n. Moreover, the width of the double capture Gaussian curves increases with increasing n and, in turn, at high projectile charges (Fig. 3). As mentioned above, similarly to single electron capture, double electron capture at v

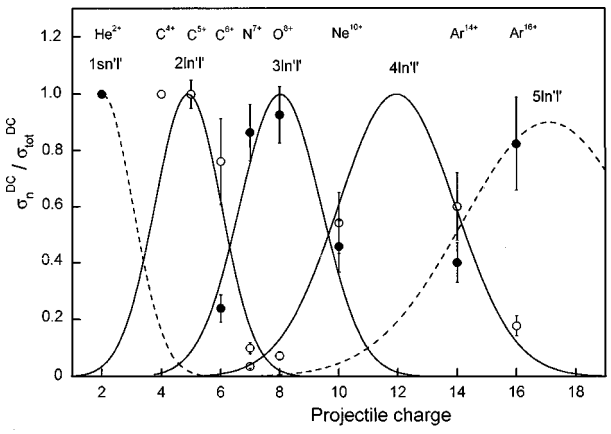

FIG. 3. Experimental ratios $\sigma_n^{\mathrm{DC}}/\sigma_{\mathrm{tot}}^{\mathrm{DC}}$ for double electron capture as a function of the projectile charge in $A^{q+}+\mathrm{He}$ collisions at the velocity $v\approx 0.5$ a.u. (odd n, solid circles; even n, open circles). The quantity σ_n^{DC} is defined as the sum over quantum numbers n', l, l' of cross sections $\sigma_{nln'l'}^{\mathrm{DC}}$ for producing configurations $nln'l'$. Gaussian curves (solid lines) are used to fit experimental data. Dashed Gaussian lines extrapolate experiment for $n=1$ and 5. The data are taken from the following references: $q=2$ [51], $q=4$ [42], $q=5$ [52], $q=6$ [8], $q=7$ (present results), $q=8$ (present results and Ref. [43]), $q=10$ [17], and $q=14,16$ (present results).

TABLE IV. Experimental cross sections σ_n^{DC} ($n=2-4$) for producing a given n state relative to total double capture cross sections σ_{tot}^{DC} in $A^{q+}+He$ collisions ($q=5-8$) at the velocity $v\approx 0.5$ a.u. In the last row, the total double capture cross sections σ_{tot}^{DC} deduced from the scaling law formulated in Ref. [25] is given. $q=5$ [42], $q=6$ [8], and $q=7,8$ (present results).

	$\sigma_n^{DC}/\sigma_{tot}^{DC}$			
n	$q=5$	$q=6$	$q=7$	$q=8$
2	1.0	0.76	0.10	0
3	0	0.24	0.86	0.93
4	0	0	0.04	0.07
σ_{tot}^{DC} (10^{-16} cm^2)	5.1	6.2	7.2	8.2

$=0.5$ a.u. is mainly caused by monoelectronic processes due to independent electron-nucleus interaction, populating predominantly configurations of (nearly) equivalent electrons $nln'l'$ ($n'\approx n$) [17,20]. The observation of similarities between single and double capture at $v=0.5$ a.u. (see Figs. 2 and 3) can be explained by the dominance of monoelectronic processes.

B. Partial double capture cross sections $\sigma_{n,n'}^{DC}$

Based on the success of the scaling law (2) to represent the charge distributions for single and double capture at a velocity of 0.5 a.u., we turn our attention to the partial cross sections $\sigma_{n,n'}^{DC}$ for producing the configurations $nln'l'$ (summed over l and l'). As mentioned above, due to the dominance of monoelectronic processes at this velocity, double electron capture can be treated as two independent single captures. Hence, for a given n value, a similar behavior is expected for the charge distribution of the partial cross sections $\sigma_{n,n'}^{DC}$.

Partial cross sections $\sigma_{n,n'}^{DC}$ relative to total cross sections σ_{tot}^{DC} are shown in Fig. 4 as a function of the projectile charge, at the impact velocity of ~ 0.5 a.u. The quantity σ_{tot}^{DC} is defined as above (Sec. III A), i.e., σ_{tot}^{DC} is the sum of the cross sections $\sigma_{n,n'}^{DC}$ over n and n'. Charge distributions for the configurations $2ln'l'$ and $3ln'l'$ ($n'=n-n+2$) are derived from experiment [8,18,42,43]. It is noted that the number of experimental data for partial cross sections $\sigma_{n,n'}^{DC}$ is rather small. For the particular case of $4ln'l'$ (bottom of Fig. 4) no experimental data are available for q values larger than 10. Hence no attempt was made to formulate a scaling law for the configurations presented in Fig. 4.

TABLE V. Values of the fitting parameters q_{max} and Δq of the Gaussian curves [Eq. (2)] characterizing the charge distribution in double capture for $A^{q+}+He$ collisions (Fig. 2) at projectile velocities of 0.5 a.u., as a function of the principal quantum number n populated during the collision. The value of unity was taken for the amplitude $a_0(n)$ (see the text). The uncertainties result from the standard deviation of the fitting procedure.

n	q_{max}	Δq
1	2	1.5
2	4.9 ± 0.2	1.6 ± 0.3
3	8.3 ± 0.1	2.0 ± 0.5
4	12.3 ± 0.1	2.7 ± 0.4

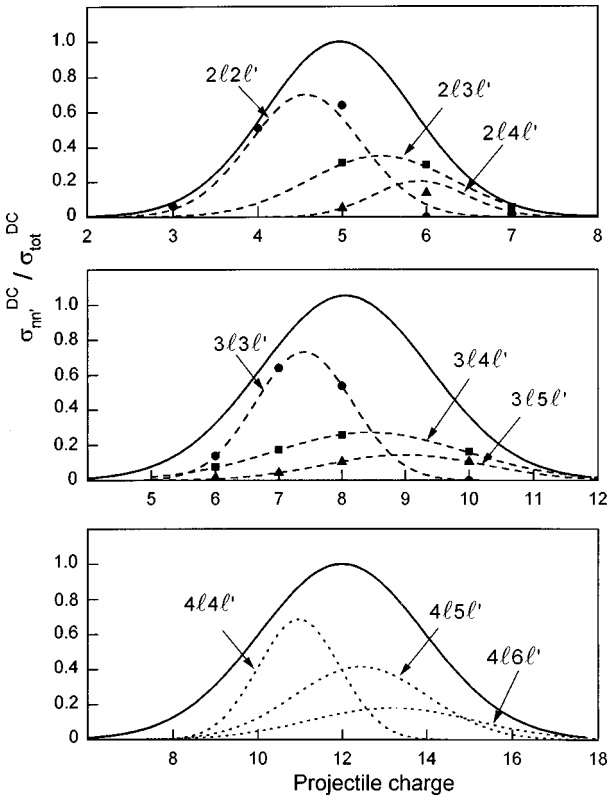

FIG. 4. Experimental ratios $\sigma_{n,n'}^{DC}/\sigma_{tot}^{DC}$ for double electron capture as a function of the projectile charge in $A^{q+}+He$ collisions at velocities of $v\approx 0.5$ a.u. The experimental data for $n=2$ and 3 are presented in the top and middle figures, respectively ($n'=n$, ●; $n'=n+1$, ■; $n'=n+2$, ▲). For each complex (n,n'), Gaussian curves are used to fit the experimental ratios (dashed curves). In addition, for each n value, the solid curve exhibits the expected sum over n' of the ratios $\sigma_{n,n'}^{DC}/\sigma_{tot}^{DC}$ that are derived from the Gaussian curves given in Fig. 3. The data are taken from the following references: $q=5$ [42], $q=6$ [8], $q=7,8$ (present results), and $q=10$ [18].

However, to visualize the dependence with respect to the projectile charge, Gaussian curves were used to fit the experimental ratios $\sigma_{n,n'}^{DC}/\sigma_{tot}^{DC}$ for each configuration $2ln'l'$ and $3ln'l'$ (dashed lines in Fig. 4). A reproducible behavior is observed. Similarly to single electron capture, the higher the projectile charge, the higher the principal quantum number n' (for a given n) of the populated states. Thus configurations of equivalent electrons $nln'l'$ ($n=n'$) are dominant for $q\leqslant q_{max}(n)$, whereas the population of configurations $nln'l'$ with $n'\geqslant n+1$ increases for higher charges.

To allow a further discussion for the configurations $4ln'l'$, approximate Gaussian curves that are similar to those found for the configurations $2ln'l'$ and $3ln'l'$ were plotted (bottom of Fig. 4). Within the series $4ln'l'$ ($n'\geqslant 4$), it is seen that the configurations $4l4l'$ are expected to be predominantly populated for charges smaller than $q_{max}(4)\approx 12$. Thus the ratio $\sigma_{4l4l'}^{DC}/\sigma_{4l5l'}^{DC}$ is likely to be noticeably larger than unity in $Ne^{10+}+He$ collisions at an im-

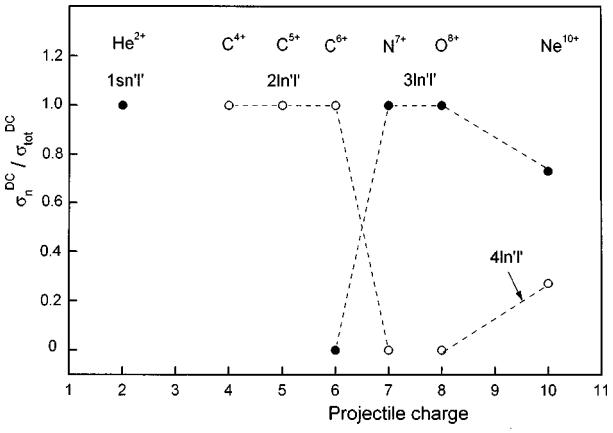

FIG. 5. Experimental ratios $\sigma_n^{DC}/\sigma_{tot}^{DC}$ for double electron capture as a function of the projectile charge in $A^{q+}+He$ collisions at velocities of $v \approx 0.1$ a.u. (odd n, solid circles; even n, open circles). Dashed lines are to guide the eye. The data are taken from the following references: $q=2$ [51], $q=4$ [22], $q=5$ [52], $q=6$ [22,53], $q=7,8$ (present results), and $q=10$ [18].

pact velocity of 0.5 a.u. Recently, this qualitative expectation has been confirmed in Auger electron spectroscopy [22] and recoil-ion-momentum spectroscopy [44,45] measurements, where a value of $\sigma_{4l4l'}^{DC}/\sigma_{4l5l'}^{DC} \sim 2$ was found. Experimental and theoretical works are suggested to provide more quantitative information on partial cross sections $\sigma_{n,n'}^{DC}$.

C. Charge distribution at 0.1 a.u.

At a velocity of ~ 0.1 a.u., the charge distributions drastically change, as shown in Fig. 5. Despite the small number of experimental data, this figure shows some significant features. First, double electron capture becomes strongly selective, giving rise to ratios $\sigma_n^{DC}/\sigma_{tot}^{DC}$ as large as unity when favoring a unique configuration series $nln'l'$ (defined for a given n value). Also, the $2ln'l'$ and $3ln'l'$ series are produced with a probability close to unity in a wide projectile charge range. However, very strong charge dependences are observed in restricted charge ranges. For example, in going from charge state 6 to 7, the ratio $\sigma_2^{DC}/\sigma_{tot}^{DC}$ nearly vanishes, whereas $\sigma_3^{DC}/\sigma_{tot}^{DC}$ increases from nearly 0 to unity.

This specific selectivity observed for double electron capture at $v=0.1$ a.u. is caused by the dominance of dielectronic processes at very low impact energies. In particular, as suggested in the discussion of Fig. 1 for the example of a projectile charge of 6, the emergence of dielectronic processes favors the production of *nonequivalent* electron configurations $nln'l'$ with n' values noticeably larger than n. While such configurations were shown to be slightly populated at velocities larger than 0.5 a.u. [20], they were found experimentally to become dominant in very slow collisions. For example, in $C^{6+}+He$ collisions, the cross sections for producing the configurations $2ln'l'$ $(n' \geqslant 6)$ noticeably increase with decreasing projectile velocity [20]. The same result was recently found for the $O^{6+}+He$ system [46], where a strong enhancement of cross sections for the production of the configurations $2pn'l'$ $(n' \geqslant 6)$ was observed when the velocity decreases. Similarly, in $Ne^{10+}+He$ collisions, relative cross sections for populating configurations $4ln'l'$ $(n'=4,5)$ significantly decrease in favor of the configurations $3ln'l'$ $(n' \geqslant 6)$ [22] for very low velocities. For this system, the cross section for populating the configurations $3ln'l'$ $(n' \geqslant 6)$ was found to be about three times larger than that for populating the configurations $4ln'l'$ $(n'=5,6)$.

In Fig. 5 it is seen that Gaussian curves are unlikely to fit the experimental data for charges up to 10. Therefore, no simple scaling law is possible at this low velocity. Nevertheless, it should be recalled that similarities occur with the $C^{6+}+He$, $Ne^{10+}+He$, and $Ar^{14+}+He$ systems at $v=0.5$ a.u. (see Fig. 3). At this higher velocity, the double-capture data points for collisions of C^{6+}, Ne^{10+}, and Ar^{14+} on He are all on the right-hand sides of the $2ln'l'$, $3ln'l'$, and $4ln'l'$ Gaussian curves, respectively. Therefore, it would be interesting to investigate the $Ar^{14+}+He$ system at $v=0.1$ a.u. so as to confirm the enhancement of the nonequivalent electron configurations $4ln'l'$ $(n' \gg n)$ when a projectile charge as high as 14 is used.

IV. CONCLUSION

Empirical scaling rules for single and double electron capture from a He target were obtained. Partial cross sections relative to total cross sections were studied as a function of the projectile charge at velocities of about 0.1 and 0.5 a.u. This work complements systematic studies of total cross sections in the case of collisions between highly charged ions and atomic targets [23–25].

For single capture, the formulated scaling law is nearly the same at projectile velocities of 0.1 and 0.5 a.u. At $v=0.5$ a.u., good agreement was found between Landau-Zener model calculations and the experimental scaling law. This agreement suggests that the fitting constants (Table III) can be applied to high projectile charges $(q>20)$ as well to predict with good approximation the corresponding cross section ratios $\sigma_n^{SC}/\sigma_{tot}^{SC}$.

Similar techniques were applied to double electron capture at velocities of 0.1 and 0.5 a.u. An important velocity dependence was observed for the cross section ratios $\sigma_n^{DC}/\sigma_{tot}^{DC}$ due to the mechanisms that govern double capture. First, at a projectile velocity of 0.5 a.u., the charge distributions were found to be close to those for single charge transfer and a scaling law was extracted from the experimental data. Furthermore, production of the configurations $nln'l'$ $(n' \leqslant n+2)$ for a given n value was found to be similar to that for single electron capture. These similarities were related to the double capture mechanisms. Due to the dominance of monoelectronic processes (electron-nucleus interactions) at 0.5 a.u., double electron capture was considered as two independent single capture events. Therefore, since the He-target electrons occupy initially a configuration of equivalent electrons $1s^2$, configurations $nln'l'$ $(n' \leqslant n+2)$ of nearly equivalent electrons are predominantly populated at $v=0.5$ a.u.

At the impact velocity of 0.1 a.u., the charge distributions for double capture change due to the emergence of dielectronic processes. These processes lead to a specific selectivity, favoring the production of nonequivalent electron configurations $nln'l'$ $(n' \gg n)$ [22]. Consequently, the

similarities at $v = 0.1$ a.u. between single and double electron capture vanish and no simple scaling rule could be derived for the projectile charges investigated experimentally ($q \leqslant 10$). More experiments in a wider range of projectile energies are needed to better describe the velocity dependence of double electron capture.

It is noted that the electron-nucleus interaction is enhanced with increasing projectile charge. Hence, for the case of very low impact velocities, the investigation of double electron capture using higher projectile charges (q ranging from 11 up to 20) is suggested to study the competition between the electron-nucleus interaction (monoelectronic processes) and the electron-electron interaction (dielectronic processes). In particular, it would be of considerable importance to verify the production of nonequivalent electron configurations at 0.1 a.u. when ion charges significantly larger than 10 are used.

ACKNOWLEDGMENTS

We gratefully thank J. A. Tanis and N. Stolterfoht for their comments on the manuscript. (J.-Y.C.) is much indebted to the Alexander von Humboldt Foundation (Germany) for its support.

[1] K. W. Gentle, Rev. Mod. Phys. **67**, 809 (1995).
[2] M. Pieksma, M. Gargaud, R. McCaroll, and C. C. Havener, Phys. Rev. A **54**, R13 (1996).
[3] C. Harel, H. Jouin, and B. Pons, J. Phys. B **24**, L425 (1991).
[4] Z. Chen, R. Shingal, and C. D. Lin, J. Phys. B **24**, 4215 (1991).
[5] L. Folkerts, M. A. Haque, C. C. Havener, N. Shimakura, and M. Kimura, Phys. Rev. A **51**, 3685 (1995).
[6] S. Bliman, A. Bárány, M. Bonnefoy, J. J. Bonnet, M. Chassevent, A. G. Fleury, D. Hitz, E. J. Knystautas, J. Nordgren, J. E. Rubensson, and M. G. Suraud, J. Phys. B **25**, 2065 (1992).
[7] A. Bordenave-Montesquieu, P. Moretto-Capelle, A. Gonzalez, M. Benhenni, H. Bachau, and I. Sánchez, J. Phys. B **27**, 4243 (1994).
[8] N. Stolterfoht, K. Sommer, J. K. Swenson, C. C. Havener, and F. W. Meyer, Phys. Rev. A **42**, 5396 (1990).
[9] R. K. Janev and H. Winter, Phys. Rep. **117**, 265 (1985).
[10] P. Boduch, M. Chantepie, D. Hennecart, X. Husson, H. Kucal, D. Lecler, and I. Lesteven-Vaisse, J. Phys. B **27**, 3079 (1994).
[11] P. Roncin, C. Adjouri, N. Andersen, M. Barat, A. Dubois, M. N. Gaboriaud, J. P. Hansen, S. E. Nielsen, and S. Z. Szilagyi, J. Phys. B **27**, 3079 (1994).
[12] J. P. M. Beijers, R. Hoekstra, A. R. Schlatmann, R. Morgenstern, and F. J. de Heer, J. Phys. B **25**, 463 (1992).
[13] R. K. Janev, L. P. Presnyakov, and V. P. Shevelko, *Physics of Highly Charged Ions* (Springer-Verlag, Heidelberg, 1985).
[14] A. Niehaus, J. Phys. B **19**, 2925 (1986).
[15] V. N. Ostrovsky, J. Phys. B **24**, 4553 (1991).
[16] C. Harel and H. Jouin, J. Phys. B **25**, 221 (1992).
[17] F. Frémont, H. Merabet, J.-Y. Chesnel, X. Husson, A. Lepoutre, D. Lecler, and N. Stolterfoht, Phys. Rev. A **50**, 3117 (1994).
[18] J.-Y. Chesnel, H. Merabet, F. Frémont, G. Cremer, X. Husson, D. Lecler, G. Rieger, A. Spieler, M. Grether, and N. Stolterfoht, Phys. Rev. A **53**, 4198 (1996).
[19] M. Barat and P. Roncin, J. Phys. B **25**, 2205 (1992).
[20] J.-Y. Chesnel, H. Merabet, X. Husson, F. Frémont, D. Lecler, C. Harel, H. Jouin, and N. Stolterfoht, Phys. Rev. A **53**, 2337 (1996).
[21] N. Stolterfoht, C. C. Havener, R. A. Phaneuf, J. K. Swenson, S. M. Shafroth, and F. W. Meyer, Nucl. Instrum. Methods Phys. Res. B **27**, 584 (1987).
[22] J.-Y. Chesnel, B. Sulik, H. Merabet, C. Bedouet, F. Frémont, X. Husson, M. Grether, A. Spieler, and N. Stolterfoht, Phys. Rev. A **57**, 3546 (1998).
[23] A. Müller and E. Salzborn, Phys. Lett. **62A**, 391 (1977).
[24] T. Iwai, Y. Kaneko, M. Kimura, N. Kobayashi, S. Ohtani, K. Okuno, S. Takagi, H. Tawara, and S. Tsurubuchi, Phys. Rev. A **26**, 105 (1982).
[25] N. Selberg, C. Biedermann, and H. Cederquist, Phys. Rev. A **54**, 4127 (1996).
[26] As shown previously for the O^{6+} and Ne^{8+}+He systems, for example [16], the presence of a $1s^2$ core weakly affects cross sections for single and double electron capture, so that the condition $q \geqslant Z-2$ is justified.
[27] L. D. Landau, Phys. Sovietunion **2**, 46 (1932); C. Zener, Proc. R. Soc. London, Ser. A **137**, 696 (1932).
[28] H. Suzuki, Y. Kajikawa, N. Toshima, H. Ryufuku, and T. Watanabe, Phys. Rev. A **29**, 525 (1984).
[29] W. Fritsch, J. Phys. B **27**, 3461 (1994), and references therein.
[30] I. Wirkner-Bott, W. Seim, A. Müller, P. Kester, and E. Salzborn, J. Phys. B **14**, 3987 (1981).
[31] D. Dijkkamp, A. Brazuk, A. G. Drentje, F. J. de Heer, and H. Winter, J. Phys. B **16**, L343 (1983).
[32] D. Dijkkamp, D. Ciric, E. Vlieg, A. de Boer, and F. J. de Heer, J. Phys. B **18**, 4763 (1985).
[33] J. P. Hansen and K. Taulbjerg, Phys. Rev. A **47**, 2987 (1993).
[34] D. Dijkkamp, Y. S. Gordeev, A. Brazuk, A. G. Drentje, and F. J. de Heer, J. Phys. B **18**, 737 (1985).
[35] W. Wu, J. P. Giese, Z. Chen, R. Ali, C. L. Cocke, P. Richard, and M. Stöckli, Phys. Rev. A **50**, 502 (1994).
[36] A. Cassimi, S. Duponchel, X. Fléchard, P. Jardin, P. Sortais, D. Hennecart, and R. E. Olson, Phys. Rev. Lett. **76**, 3679 (1996).
[37] S. Duponchel, Ph.D. thesis, University of Caen, 1997 (unpublished).
[38] W. Fritsch and C. D. Lin, J. Phys. B **19**, 2683 (1986).
[39] C. Harel and H. Jouin, Europhys. Lett. **11**, 121 (1990).
[40] A. Bordenave-Montesquieu, P. Benoit-Cattin, A. Gleizes, A. I. Marrakchi, S. Dousson, and D. Hitz, J. Phys. B **17**, L127 (1984).
[41] X. Fléchard, L. Adoui, A. Cassimi, S. Duponchel, and D. Hennecart (private communication).
[42] H. A. Sakaue, Y. Awaya, A. Danjo, T. Kambara, Y. Kanai, T. Takayanagi, K. Wakija, Y. Yamada, and M. Yoshino, J. Phys. B **24**, 3787 (1991).
[43] M. Mack, J. H. Nijland, P. van der Straten, A. Niehaus, and R. Morgenstern, Phys. Rev. A **39**, 3846 (1989).
[44] X. Fléchard, S. Suponchel, L. Adoui, A. Cassimi, P. Roncin, and D. Hennecart, J. Phys. B **30**, 3697 (1997).

[45] M. Abdallah and C. L. Cocke (private communication).
[46] A. Spieler, M. Grether, and N. Stolterfoht (private communication).
[47] V. V. Afrosimov, A. A. Basalaev, G. A. Leiko, and M. N. Panov, Zh. Eksp. Teor. Fiz. **74**, (1978).
[48] H. Tawara, T. Iwai, Y. Kaneko, M. Kimura, N. Kobayashi, A. Matsumoto, S. Ohtani, K. Okuno, S. Takagi, and S. Tsurubushi, Phys. Rev. A **29**, 1529 (1984).
[49] H. Cederquist, C. Biedermann, and N. Selberg, Phys. Rev. A **51**, 2169 (1995).
[50] A. L. Lopez-Castillo and F. R. Ornellas, Phys. Rev. A **51**, 381 (1995).
[51] J. E. Bayfield and G. A. Khayallah, Phys. Rev. A **11**, 920 (1975).
[52] R. Mann, Phys. Rev. A **35**, 4988 (1987).
[53] M. Barat, M. N. Gaboriaud, L. Guillemot, P. Roncin, H. Laurent, and S. Andriamonje, J. Phys. B **20**, 5771 (1987).